Research article

Behavior of heat damaged reinforced recycled aggregate concrete beams repaired with NSM-CFRP strips

W.S. Barham ✉️ iD **, Y.T. Obaidat** iD **, H.A. Alkhatatbeh** iD

Jordan University of Science and Technology, Irbid, Jordan

✉️ *wsbarham@just.edu.jo*

Abstract. The behavior of heat damaged Recycled Aggregate Concrete (RAC) beams repaired with NSM-CFRP strips is the subject of this experimental study. The effect of heat damage on the RAC beams and the post-heating residual strength of beams were studied and compared with natural beams. Different volumetric percentages (0 %, 25 % and 50 %) of coarse Recycled Concrete Aggregates (RCA) were used in three concrete mixes (N, R25 and R50), producing a total of 16 reinforced beams having the same cross-section (100 mm×150 mm×1150 mm). Specimens were exposed to two levels of heat, 25 °C at ambient air and 400 °C for a three-hour period. The post-heating residual strength of RAC beams was studied and compared with natural ones. The flexural test conducted indicated a reduction in the load carrying capacities and stiffness due to mechanical deterioration in concrete properties and bond strength. The reduction in stiffness increased as RCA content increased due to a large amount of weak decomposed cement mortar in the RAC. The NSM-CFRP strips technique was used with epoxy adhesive for strengthening/recovering the flexural capacities of intact/ heat-damaged RAC beams. Four groups of simply supported beams were tested in a four-point bending test; the enhancement/reduction in strength and the mechanical properties were recorded. Results indicated that strengthened beams showed comparable behavior with those made with conventional concrete at room temperature. On the other hand, the behavior of repaired beams after being exposed to 400 °C showed different failure modes depending on the RCA percentage and the repairing configurations. RAC with higher RCA replacement ratio has a lower bond strength and therefore, a larger slippage was reported. The weak bond between the epoxy adhesive and the surrounding concrete caused the reduction in stiffness. Finally, using NSM CFRP with two strips at the sides (one strip at each side) for strengthening and repairing of intact/heat-damaged RAC beams resulted in slight improvement of the load carrying capacities. It reduced the induced strain in the CFRP strips to about 40 % of its value when a single concentrated strip at the bottom is used, and minimizing the slippage due to lower stresses and strains in the CFRP strips.

1. Introduction

Concrete recycling has become an alternative solution to use concrete debris rather than routinely trucking it to landfills for disposal [1]. Recently, the structural applications of recycled aggregate concrete have become a field of interest for engineers and scientists. Therefore, the strengthening and repairing of recycled concrete structures became a necessity. These structures may need to be enhanced or rehabilitated because they are in a weakened state, not only due to deterioration, but also due to errors

that could be committed in the design and execution processes. Therefore, repairing or strengthening of the existing structures may be needed whenever the structural members are damaged. Experimental studies conducted on the field of concrete materials recycling concluded the possibility to transform the concrete waste into good quality recycled concrete aggregate to be used in the concrete industry. The recycled concrete aggregates possess lower specific gravity, bulk density, and resistance against mechanical action including impact load and crushing value, but higher water absorption capacity and porosity when compared with the natural ones. This is due to the presence of low-density cement paste adhered to the old aggregate [2–5]. These properties are strongly affected by the strength of the parent concrete [6]. Moreover, any gradation could be achieved with recycled aggregate by monitoring the crushing process. However, the crushing may produce some residual dust on the coarse aggregate surfaces, and hence washing it becomes essential.

Many studies were conducted to evaluate damage in the recycled aggregate concrete in terms of its mechanical properties and stress-strain relationships. Although most of the studies showed properties of concrete degrade as the level of exposure temperature rises, the post-heating and post-fire mechanical behavior of recycled aggregate concrete was satisfactory and comparable with the natural concrete [6–10]. Moreover, the elastic modulus of recycled aggregate concrete degraded with an increase in recycled aggregate content at any level of heat exposure [7–9, 12], whereas the peak strain increased [10]. Also, recycled aggregate concrete shows adequate thermal compatibility, since no spalling or fragmentation of the specimen was noticed when heated [7, 9, 13]. Finally, it is worth to point out that recycled aggregate concrete with higher replacement ratio and lower w/c ratio behaves better than the natural concrete upon heating due to thermal compatibility of the old and new cement mortars, therefore, the effect of the high temperatures in this zone is less important [12]. The principal results of successive bending tests conducted over years showed flexural strength of recycled and natural aggregate concrete beams are considered the same for the service and ultimate loading [14–17]. However, the cracking moment is significantly affected by the recycled concrete aggregate content as well as the maximum cracks propagation and deflection under serviceable load [14, 18]. On the other hand, the increase in recycled aggregate content leads to an increase in the ultimate flexural deflections and a decrease in the initial stiffness [19].

Fiber-reinforced polymer composites (FRP) is one of the discoveries that received a positive acceptance from civil engineers for strengthening and repairing of structures [20–23]. One of the essential techniques that has been used is carbon fiber reinforced polymer (CFRP) in a polymeric matrix fabricated into different forms, such as plates, strips, or flexible sheets. CFRP can be bonded to the outer face of the RC element using high strength epoxy or cement mortar, known as externally bonded, or installed into grooves cut into the RC element in the predetermined direction, known as Near Surface Mounted (NSM) technique. The last becomes particularly attractive for flexural and shear strengthening for different structural elements [24, 25]. Research conducted indicated that Externally Bonded Reinforcement (EBR) has lower efficiency than NSM technique due to debonding of FRP material. In addition, FRP material, in the case of the EB technique, is vulnerable against physical damage, fire facing, thermal changes, and ultraviolet radiation [26-29]. All the experiments implemented with NSM FRP technique have proved its effectiveness in enhancing flexural capacity of structural members. Beams strengthened with NSM technique showed a rise in flexural capacity at different percentages with respect to control beam depending on the type of failure [30, 31]. The failure mode of RC with NSM CFRP is dependent on different parameters. Two types of rupture are possible for NSM systems. These are pull-out and peeling off [32]. Debonding is another common failure mode, which occurs in different ways: bond failure at the CFRP-adhesive interface, adhesive-concrete interface, splitting of adhesive cover, concrete cover separation, and secondary debonding failure mechanisms [33]. Usually, debonding failure occurring at the CFRP–adhesive or the adhesive–concrete interfaces control the failure of beams strengthened with EBR CFRP strips, whereas the failure of beams strengthened with NSM CFRP strips is controlled by debonding of CFRP strips and cover separation by peeling off the CFRP strips together with the concrete cover [27].

The bond behavior and its characteristics represent a key issue in evaluating the structural performance of the strengthening/repairing systems. Many factors could affect the bond and the local bond-slip behavior of these strengthening/repairing systems, including mechanical properties of constituent materials, surface state of the FRP reinforcement, and finally, the geometry of grooves. The lack of bond between FRP and concrete beams will cause serious problems and lead to different modes of failure. In the NSM FRP method, certain types of failure have been observed during the experiments, including flexure and debonding failure. The former is caused by the yielding of steel bars accompanying concrete crushing or FRP rupture [34, 35]. In addition to the above-stated factors, the test set-up used has a significant effect on both the bond-slip relationship and the debonding load [36–38]. This research aims to explore the effect of using RAC in the flexural behavior of unheated and heat-damaged beams, to investigate the effect of using CFRP NSM strips in the flexural capacity of the RAC beams, and finally, to examine its effect on increasing/recovering the capacity and failure modes of heat-damaged beams.

2. Methods

2.1. Material properties

2.1.1 Constituent materials of the concrete

All concrete mixtures were produced using type I ordinary Portland cement (CEM I 42.5). Two types of coarse aggregate with maximum aggregate size of 19 mm, were used: natural crushed limestone and Recycled Concrete Aggregate (RCA). In addition, a blend of fine crushed limestone and natural silica sand (75 % fine crushed limestone and 25 % silica sand) was used. Tap water was used in mixing and curing of concrete. Properties of materials used in concrete were tested according to ASTM specifications [39–42] and summarized in Table 1. Coarse RCA used in this research was produced by manual crushing of waste concrete cylinders used in previous studies with parent strength concrete at 50 MPa.

Table 1. Shortlist of physical and mechanical properties of materials used in concrete.

	ASG	BSG (SSD)	BSG (OD)	Absorption %	M.C %	Dry Rodded Unit Weight (Kg/m3)	Abrasion Resistance %	F.M
Cement	3.15	–	–	–	–	3150	–	
Natural Coarse Aggregate	2.67	2.56	2.53	2.63	0.14	1502.55	25	6.86
Recycled Coarse Aggregate	2.63	2.36	2.21	7.24	2.43	1290.52	35	7.05
Natural Fine Aggregate	2.68	2.58	2.52	2.4	0.5	1922.53	–	3.12
Silica sand	2.67	2.64	2.61	0.5	0.65	2010.3	–	1.41

BSG: Bulk Specific Gravity; ASG: Apparent Specific Gravity M.C: Moisture content; F.M. Fineness Modulus.

2.1.2 Reinforcing steel

Grade 60 (yield stress = 420 MPa) deformed steel bars, 10 mm in diameter, were used for the longitudinal reinforcement, and Grade 40 (yield stress = 280 MPa) 8 mm diameter undeformed steel bars were used for transverse reinforcement (Stirrups). Steel bars used for reinforcing were tested at room temperature about 25 °C and after exposure to an elevated temperature of 400 °C for three hours; the pre and post-heating mechanical properties were determined according to ASTM A370 [43]. Table 2 shows the mechanical properties of the bars tested. Results indicated a reduction in mechanical strength of both types of steel bars upon heating, including yielding and ultimate stresses.

Table 2. Post heating mechanical properties of the reinforced steel.

Temperature	Nominal Bar Diameter (mm)	Yield Stress f_y (MPa)	Ultimate Stress f_u (MPa)
23 °C	10.2	440	625
	8.1	340	431
400 °C	10.2	426	613
	8.1	295	404

2.1.3 Carbon Fiber Reinforced Polymer and Epoxy Resin.

Unidirectional high-strength NSM-CFRP strips, manufactured by SIKA, were used in the strengthening and repairing of different specimens using epoxy resin adhesive (Sikadur -30LP). Epoxy resin was used as bonding adhesive to fill the grooves and glue the strips to the concrete surface. This adhesive was prepared from two parts: 4.5 kg of white resin (part A) and black hardener (part B) with mixing proportion Resin (A): Hardener (B) = 3:1 by weight or volume to get 6 kg (A+B) light gray bonding adhesive mixture. Table 3 presents the physical and mechanical properties for the NSM-CFRP strips according to the manufacturer's reports. Table 4 presents the technical data of the epoxy adhesive.

Table 3. Physical and Mechanical Properties of Sika NSM-CFRP strips (Sika® CarboDur® S1.525).

Fiber type	High strength carbon fibers
Fiber orientation	0° (unidirectional)
Strip thickness	2.5 mm
Strip width	15 mm
Tensile E-modulus	165000 N/mm² (nominal)
Mean tensile strength	3100 N/mm²
Strain at break	> 1.7 % (nominal)

Table 4. Properties for impregnation resin (Sikadur®-30lp).

Form	Resin part A: Paste
	Hardener part B: Paste
Appearance / Colors	Part A: white
	Part B: black
	Part A+B mixed: light grey
Mixed density at 25 °C	1.8 g/cm² (approx.)
Flashpoint	N/A
Sag flow	Non-sag on vertical surface
Shrinkage	0.04 %
E-Modulus	10000 N/mm^2 (compression and tension)
Tensile strength	18 N/mm² at 7 days
Flexural strength	25 N/mm² at 7 days
Shear strength	21 N/mm² at 7 days
Compressive strength	85 N/mm² at 3 days
Bond to concrete	> 4 N/mm² at 1 day (concrete fracture)

2.2. Concrete production

Three sets of concrete mixes were designed according to the ACI-211 mix design procedure [44] with trial mixes, achieving an average cylindrical compressive strength of 37.2 MPa at 28 days. One set was natural coarse aggregate concrete (N), and the other two sets of concrete contained recycled concrete aggregate (RCA) (25 % and 50 % replacement ratios of coarse recycled concrete aggregate, volumetrically) designated as R25 and R50, respectively. All mixtures produced had uniform mixing without segregation, reflecting a good workability. For all concrete sets, the slump values measured according to ASTM C143-00 [45] were approximately in the medium range (80–120 mm). The quantities of materials are summarized in Table 5.

Table 5. Details of the concrete mixes.

Concrete Mix	Vc/Va	N.C.A (kg)	R.C.A (kg)	N.F.A (kg)	N.S (kg)	Cement (kg)	Wnet (kg)	Weff (kg)	Wnet/C	Weff/C	Slump (mm)
N	0.575	950.32	-----	533.29	185.15	372.8	234	200	0.63	0.54	115
R25	0.576	712.74	208.2	527.41	183.1	391.19	237.3	200	0.61	0.51	110
R50	0.577	475.16	416.41	521.16	180.9	410.16	240.6	200	0.59	0.49	95

Vc is volume of coarse aggregate, Va is total volume of aggregate, N.C.A is natural coarse aggregate, R.C.A is recycled coarse aggregate, N.F.A is natural fine aggregate, N.S is natural silica, Wnet is net water and Weff is effective water.

A total of eighteen concrete cylinders (150 mm in diameter and 300 mm in height) were cast and cured. Each concrete mix involved six cylinders subdivided into two subgroups based on the level of heat to be exposed to. Each subgroup contained three cylinders tested according to ASTM [46] to determine the average concrete compressive strength (fc') at ambient temperature (25 °C) and after being exposed to heat (400 °C) for 3 hours in the electric furnace. In order to get accurate results from the testing machine, the cylinders were capped with sulfur to level surfaces. The average compressive strength was measured and recorded for the cylindrical specimens as illustrated in Table 6.

Table 6. Average ultimate compressive strength of different concrete mixes at different levels of heat exposure.

Concrete Mix	$f'c$ (MPa)	
	25 °C	400 °C
N	37.1	29.92
R25	38.2	29.81
R50	37.5	27.80
Average	37.6	29.2

$f'c$ is 28-day compressive cylinder strength of concrete

2.3. Specimens and beam fabrication

The study program involved sixteen reinforced concrete beams (100×150×1150 mm) designed to be under-reinforced by following the guidelines of the ACI committee 318 [47]. All beams were provided with typical longitudinal and transverse steel reinforcements. The bottom (tension) reinforcement consists of two Φ10 bars, the same as the top (compression), running along the full span of the beam. Also, the transverse shear reinforcement was roughly designed according to the ACI committee 318 [47] taking into account both the additional rise in ultimate load capacity due to the application of NSM-CFRP strips and the low shear resistance of the heat-damaged recycled aggregate concrete beams. The shear reinforcement consisted of closed 8 mm undeformed steel stirrups, distributed along the shear span and spaced 50 mm centers apart. The steel reinforcements were provided with concrete cover spacers (25 mm) at the bottoms and sides to ensure sufficient cover, then placed in the wooden formworks, as shown in Fig. 1. Specimens were divided into three main groups based on the concrete mix cast. Each group of specimens was cast with a specific concrete mix (N: natural aggregate, R25: 25 % recycled aggregate and R50: 50 % recycled aggregate) and moist-cured for 28 days. Each group was also subdivided into three sets in terms of the level of temperature exposure (25 °C at ambient air, and 400 °C).
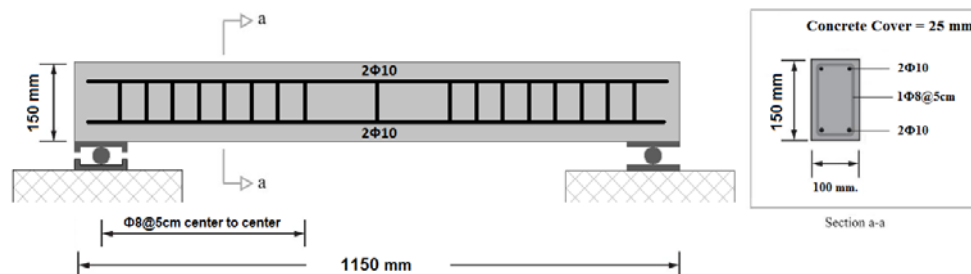
Figure 1. Specimens and beam fabrication.

2.4. Thermal treatment

Concrete specimens (beams and cylinders) were subjected to elevated temperatures using the electrical furnace available at the structural laboratory. The specimens were exposed to 400 °C (T400) heat for 3 hrs. The rate of heating is shown in Fig. 2.
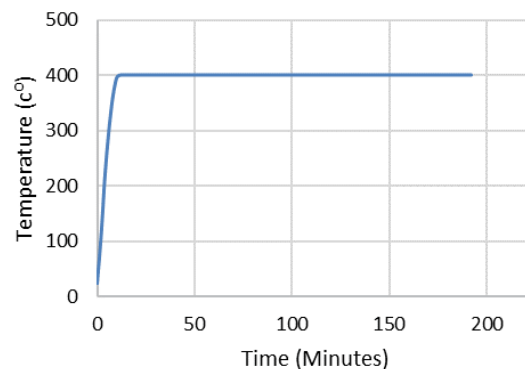
Figure 2. Temperature history of heated specimens.

2.5. Applying the NSM-CFRP strips

Finally, each set contained an unrepaired beam used as a control specimen, designated with the symbol (C), and a repaired or strengthened beam using NSM-CFRP strips. Two configurations were used for strengthening/repairing: single strip centered at the bottom or double strip at sides (one strip at each side). Each configuration was designated with the symbol S1: One strip at bottom, or S2: Two strips at both sides, respectively. Fig. 3 (a and b) shows a schematic drawing of the repairing configurations. Table 7 illustrates the characteristics of different specimens.
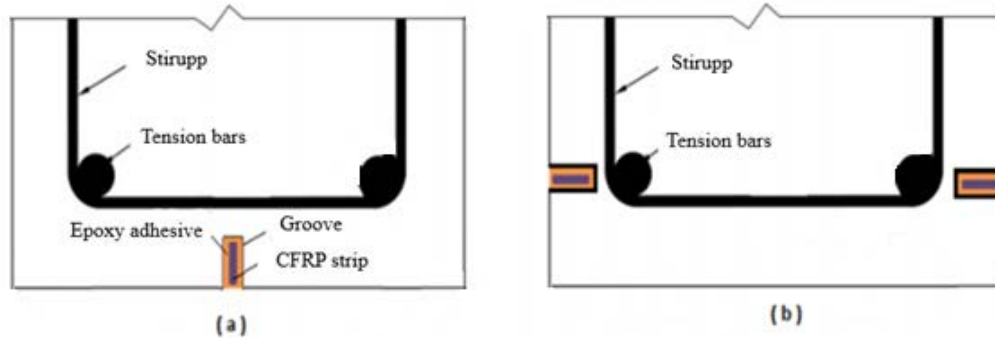
Figure 3. A schematic drawing of the repairing configurations:
(a) Single concentrated strip at soffit (S1), (b) Two strips at sides, one strip at each side (S2).

Table 7. Test program and specimens' designations.

Specimen Designation	Type of Concrete	Replacement Ratio %	Temperature (°C)	Repairing Configuration
B-N-T25-C	Natural	0	25	Control
B-N-T25-S1			25	One strip at bottom
B-N-T25-S2			25	Two strips at sides
B-N-T400-C			400	Control
B-N-T400-S1			400	One strip at bottom
B-N-T400-S2			400	Two strips at sides
B-R25-T25-C	RAC	25	25	Control
B-R25-T25-S1			25	One strip at bottom
B-R25-T400-C			400	Control
B-R25-T400-S1			400	One strip at bottom
B-R50-T25-C	RAC	50	25	Control
B-R50-T25-S1			25	One strip at bottom
B-R50-T25-S2			25	Two strips at sides
B-R50-T400-C			400	Control
B-R50-T400-S1			400	One strip at bottom
B-R50-T400-S2			400	Two strips at sides

2.6. Bonding NSM-CFRP strips

For installing the NSM CFRP strips, 25 mm depth and 8 mm width slits were cut using an electric drill for the considered configurations. Slit geometry was considered in this study to fit the dimensions of the CFRP strip employed. The slits were cleaned by an electric air blower before washed with a volatile liquid (thinner) to remove the suspended dust and reduce surface humidity. Later, the bonding adhesive was manually squeezed into the slits filling them completely using a special spatula, then the NSM CFRP strips were pressed into the epoxy up to the full depth of the slits, with the excess epoxy used to finish the surfaces covering the strips. Fig. 4 shows the NSM-CFRP strips installation process.

2.7. Test setup

All beam specimens were simply supported (one end is a hinge and the other is a roller) over a span of 1.05 m on-center, then subjected to four-point loading applied through a spreader beam. The distance between two point-loads was fixed at 350 mm. Three linear variable displacement transducers (LVDT's) were used. The first one was placed beneath the beam at the mid-span center to measure deflection,

whereas the second one was positioned horizontally to measure the longitudinal strain developed in CFRP strips. The latter was mounted on two short extensions of CFRP strips glued to the main NSM CFRP strips at two points over a gauge length of 350 mm around the center of the beams. Similarly, the third LVDT recorded the end slippage 150 mm apart from the center of support attached to a small piece of CFRP strip glued to the NSM CFRP strip in a pre-cut groove in which the head of the LVDT hits the center of small plastic plate glued to concrete surface. A schematic drawing of test setup is presented in Fig. 5.

(a)
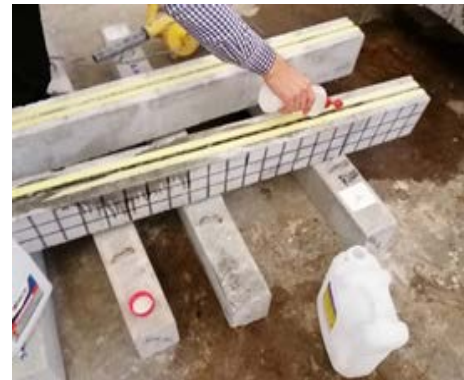
(b) Groove cleaning with thinner

(c) Filling the grooves with "epoxy" paste

(d) Installation of CFRP strips in groove

(e) Finishing the surface

(f) Strengthened/Repaired beams

Figure 4. NSM CFRP strips installation.

The load was automatically applied using a universal testing machine of 2000 KN capacity with displacement controlled at 0.041 mm/s loading rate. Using a data acquisition system, instantaneous measurements of load, mid span deflection, elongation in NSM CFRP strip, and relative slippage between the concrete and the bonded CFRP strip were automatically recorded too.
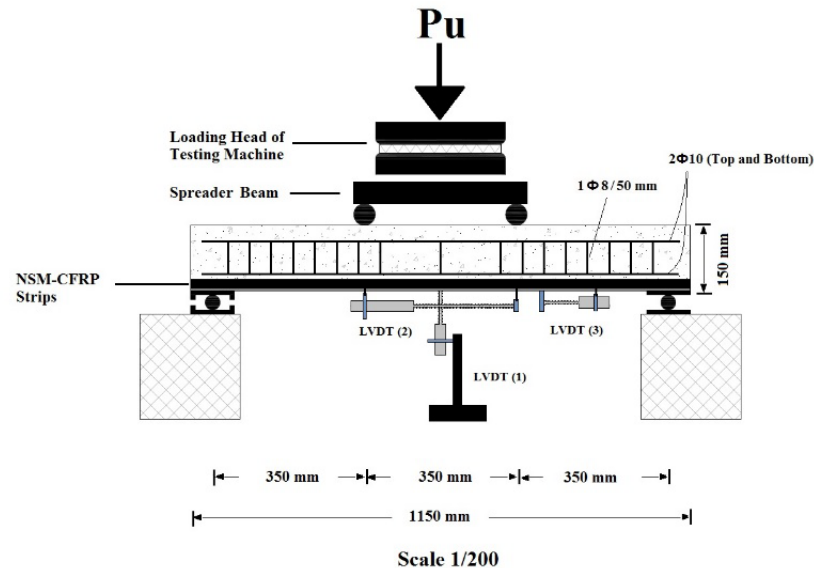
Figure 5. A schematic drawing of the test setup and LVDT's distribution.

3. Results and Discussion

The results demonstrate the post heating residual behavior of reinforced RAC beams exposed to elevated temperature and highlight the effect of NSM-CFRP strips as a strengthening/repairing method in increasing/recovering the flexural capacities of intact/heat damaged reinforced RAC beams in terms of ultimate load capacity, mid span deflection, toughness, stiffness, bond slip, and failure modes.

3.1. Load deflection stages

The load–deflection curves presented in Fig. 6, 7 and 8 can be divided into three stages: elastic stage (pre-cracking), post-cracking stage, and yield strengthening stage. In the elastic stage, the specimen's flexural stiffness is given by the uncracked section, resulting in a linear load versus displacement curve. As the load was increased above the P_{cr}, micro-cracks developed in the specimen, with noticeable cracks appearing in the weak zone of the constant bending moment region. Meanwhile, the slope of the load–displacement curve is decreasing, as can be seen in Table 9, meaning that the beam's bending stiffness is decreasing, indicating that the beam is entering the crack production stage. When the load reaches the yield load, the specimen enters the yield strengthening stage. The load increased slowly at this stage, with a large increase in displacement.

3.2. Summery of the mechanical properties of beams

Mechanical characteristics of different beams are shown below in Table 8 and 9. The results included ultimate load (Pu), ultimate deflection at mid span (Δ_u), failure mode (F.M), stiffness, and toughness, and energy adsorption. The stiffness is the slope of the linear part of the load-deflection curve. Energy adsorption is the area under the load deflection curve up to the end of the stage in consideration calculated numerically using the trapezoidal rule.

Table 8. Test results of beam specimens.

Specimen	Pu (kN)	Δu (mm)	Δy (mm)	$DI = \dfrac{\Delta u}{\Delta y}$	F.M	Max Strain in CFRP	Max Slippage (mm)
B-N-T25-C	45.15 (0.0%)[1]	13.9	4.29	3.24	F		
B-N-T25-S1	72.65 (+61%)	17.2	5.93	2.90	HC-PCS-S	0.0145	1.2519
B-N-T25-S2	74.89 (+66%)	14.3	7.37	1.94	HC-PCS-CC	0.0045	0.9867
B-N-T400-C	38.00 (-16%)	14.5	4.98	2.91	F		
B-N-T400-S1	63.46 (+41%)	26	5.3	4.91	HC-PCS-CC	0.0111	1.3947
B-N-T400-S2	65.66	12.5	5.08	2.46	F	0.0044	0.5540

Specimen	Pu (kN)	Δu (mm)	Δy (mm)	$DI = \dfrac{\Delta u}{\Delta y}$	F.M	Max Strain in CFRP	Max Slippage (mm)
B-R25-T25-C	(+45%) 44.50 (0.0%)	13.4	4.07	3.29	F		
B-R25-T25-S1	72.80 (+64%)	18.2	5.19	3.51	HC-PCS-S	0.0128	1.2965
B-R25-T400-C	36.60 (-18%)	14.9	4.02	3.71	F		
B-R25-T400-S1	63.20 (+42%)	23.5	7.11	3.31	HC-PCS-CC	0.0107	0.7960
B-R50-T25-C	44.65 (0.0%)	14.4	4.53	3.18	F		
B-R50-T25-S1	71.22 (+60%)	15.1	6.2	2.44	HC-PCS-S	0.0116	1.2965
B-R50-T25-S2	71.70 (+61%)	23.1	7.25	3.19	HC-PCS-CC	0.0043	0.3579
B-R50-T400-C	34.85 (-22%)	14.4	4.14	3.48	F		
B-R50-T400-S1	62.00 (+39%)	22.1	5.9	3.75	HC-PCS-S	0.0090	1.6580
B-R50-T400-S2	63.67 (+43%)	16.6	6.93	2.40	HC-PCS-S	0.0042	0.6200

1: Numbers between brackets represent the percentage of control specimens, +ve: increase and -ve: decrease.
F: Flexural type (Steel yielding followed by concrete crushing). DI: Ductility Index
HC-PCS-CC: Horizontal cracks cause partial cover separation with local epoxy-concrete debonding followed by concrete crushing.
HC-PCS-S: Horizontal cracks cause partial cover separation with local epoxy-concrete debonding followed by shear failure.

Table 9. Stiffness and energy absorption for the pre and post cracking stages.

Specimen	Pre-Cracking stiffness (kN/mm)	Pre-Cracking energy adsorption (kN-mm)	Pre-Yielding Stiffness (kN/mm)	Pre-yielding energy adsorption (kN-mm)	Total Energy adsorption (kN-mm)
B-N-T25-C	46.6	0.78	7.21	100	444
B-N-T25-S1	43.2	0.93	8.65	177	862
B-N-T25-S2	44.5	0.85	7.73	255	723
B-N-T400-C	29.0	0.67	6.60	110	376
B-N-T400-S1	13.6	1.73	7.80	148	562
B-N-T400-S2	14.3	2.73	8.4	135	417
B-R25-T25-C	20.6	0.91	7.50	78	430
B-R25-T25-S1	42.7	0.95	8.90	135	820
B-R25-T400-C	9.6	1.06	6.30	67	340
B-R25-T400-S1	33.5	0.64	7.70	195	536
B-R50-T25-C	31.9	0.67	7.37	97	404
B-R50-T25-S1	43.9	1.58	8.30	147	721
B-R50-T25-S2	34.0	2.50	8.97	306	969
B-R50-T400-C	16.2	0.91	5.9	69	315
B-R50-T400-S1	18.6	1.97	8.3	158	642
B-R50-T400-S2	26.5	0.65	9.3	251	446

3.3. Effect of using NSM-CFRP strips
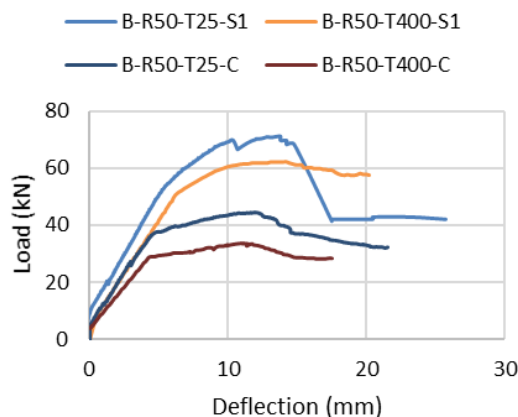### on the load-deflection response of heat-damaged beams

According to Table 8 and Fig. 6, the load-deflection curves of specimens (B-N-T400-C, B-R25-T400-C and B-R50-T400-C) showed similar trend behavior. Curves were approximately linear up to certain point before they became non-linear. The deterioration in the mechanical properties is due to the decrease in the value of yield stress for steel and deterioration of bond strength between reinforcing steel and concrete, in addition to the large decrease in the post-heating compressive strength of concrete caused by concrete degradation and thermal cracks. The stiffness of the intact concrete beams was slightly affected by the recycled concrete aggregate content, but for the heat-damaged beams, the recycled concrete aggregate content had a significant effect on the stiffness due to the weaker bond between the damaged recycled aggregate concrete and the reinforcing steel. For beams exposed to an elevated temperature of (400 °C) for three hours, results showed that a significant difference between mixes and the reduction in load capacity was relatively low due to the fact that the strength was controlled by the compressive strength of heat-damaged concrete and the yielding of the steel reinforcement. The last is not significantly affected by temperatures below 700 °C.

Fundamentally, the use of NSM CFRP strips for strengthening and repairing shows a significant enhancement in the beams' behavior including increasing the load carrying capacity as shown in Table 8 and Fig. 6. Strengthened specimens showed a similar and typical mechanical response. For example, the load carrying capacity of specimens B-N-T25-S1 and B-R50-T25-S1 were 61 % and 60 % higher than B-N-T25-C and B-R50-T25-C controlled specimens, respectively. The load-deflection curves were divided into three stages. In the first stage (elastic stage), the load increased linearly up to certain values of load and deflection, causing the initiation of the first crack in the concrete. In this stage, the bond between the CFRP strips, epoxy material, and concrete was good. In the second stage (concrete cracking to steel yielding), the curve changed its slope due to the weaker modulus of CFRP strips and steel yielding, reflecting the linear elastic response of the cracked composite section started by concrete cracking to steel yielding due to increasing bending moment. Finally, the third stage (steel yielding to failure), reflects the nonlinear behavior of the composite section.
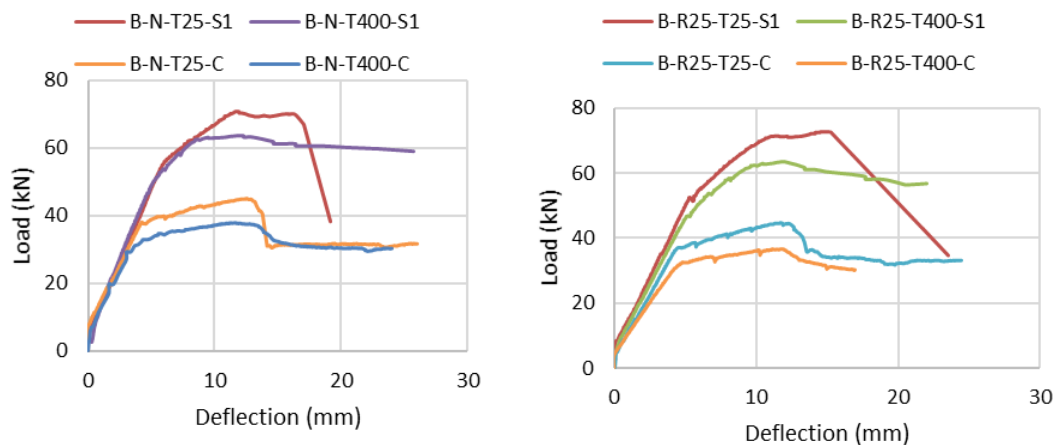
(a) Normal concrete strips

(b) R25 concrete beams

(c) R50 concrete beams
Figure 6. Effect of using NSM-CFRP strips at different levels of heat exposure.

Barham, W.S., Obaidat, Y.T., Alkhatatbeh H.A.

3.4. Effect of RAC percentage on the load-deflection response

Results showed typical behavior of beams with different percentages of recycled concrete aggregate as shown in Table 8 and Fig. 7. This is due to the strength of concrete, since all concrete mixes have the same strength regardless the recycled aggregate content indicating that Recycled Concrete Aggregate does not have an effect on the load capacity when the strength of concrete is fixed, but the deflection slightly increases as RCA increases because of the low modulus of elasticity of RAC. From Table 8, the load carrying capacity of specimens B-N-T25-C, B-R25-T25-C, and B-R50-T25-C having different RA content is almost the same.

For heat-damaged specimens at 400 °C, due to the lower tensile strength of RAC and the deterioration in mechanical properties of concrete associated with the heat-damage due to elevated temperatures, the repaired specimens exhibited comparable residual load-carrying capacities but noticeable difference for deflection as the recycled aggregate increased. On the other hand, the stiffness showed a reduction as recycled aggregate increased. For example, from Table 9, the post cracking stiffness of specimens B-N-T400-C, B-R25-T400-C, and B-R50-T400-C were 6.6 kN/mm, 6.3 kN/mm and 5.9 kN/mm, respectively.

This can be related to the significant decrease in bond strength between the damaged concrete and the epoxy adhesive as the recycled aggregate content increases. Heat-damaged recycled aggregate concrete with a high incorporation ratio of recycled concrete aggregate contains a larger amount of damaged mortar surrounding the epoxy leading to a weaker bond as shown in Fig. 7.
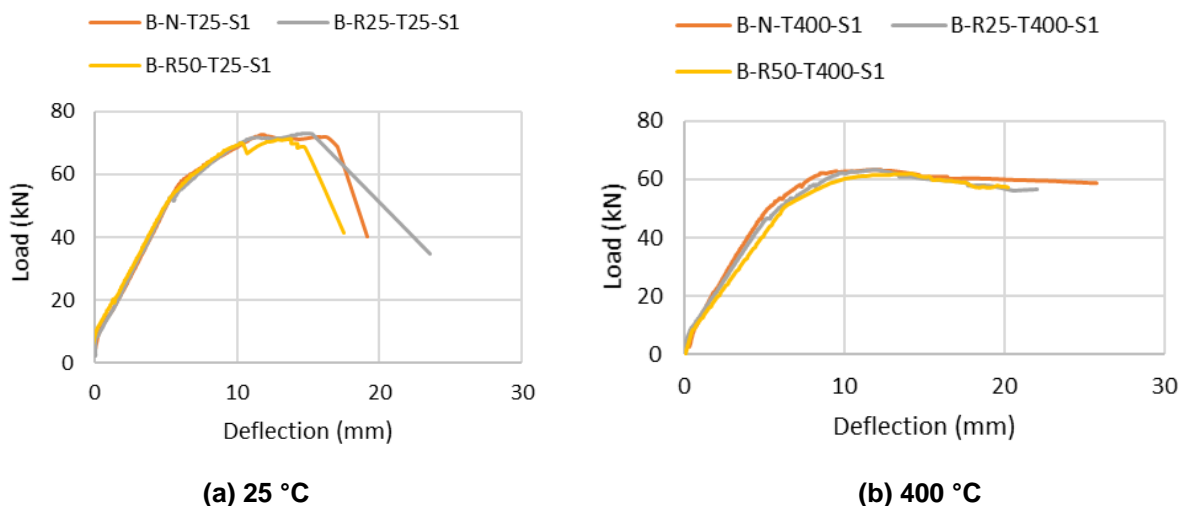

(a) 25 °C   **(b) 400 °C**

Figure 7. Effect of RAC percentage on the load-deflection response.

3.5. Effect of different strengthening/repairing configurations

In this part, the differences between strengthening/repairing configurations are discussed. Fig. 8 shows load-deflection curves of BNSM-CFRP (S1) and SNSM-CFRP (S2) for different percentages of recycled aggregate content and different levels of heat exposure. Table 8 summarizes the other parameters including stiffness and modulus. Generally, specimens strengthened/repaired with SNSM-CFRP strips (one strip at each side) showed a significant increase in the cracking load due to a higher ratio of CFRP strips. The load carrying capacity shows a slight change, however, the stiffness significantly increased but toughness decreased. In comparison with the first configuration, the second configuration indicated a significant increase in cracking load and stiffness but a significant reduction in deflection and toughness. Moreover, the ultimate load capacity does not affect the configurations.
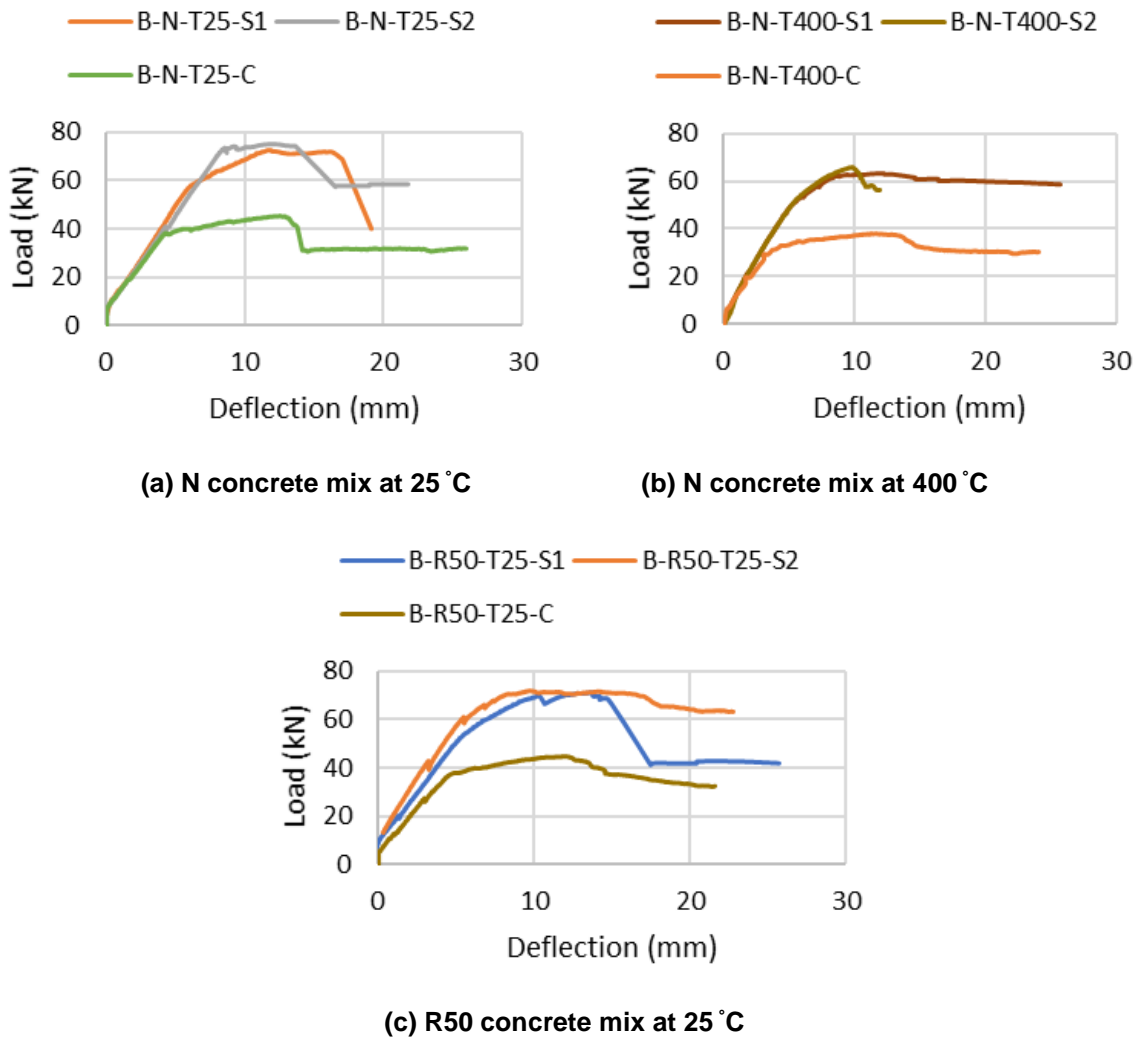
(a) N concrete mix at 25 ˚C

(b) N concrete mix at 400 ˚C

(c) R50 concrete mix at 25 ˚C

Figure 8. Effect of NSM-CFRP strips strengthening/repairing configuration.

3.6. Strain Development in NSM-CFRP Strips and Bond Slippage

3.6.1. Strain in NSM-CFRP strips

Fig. 9 shows that the induced strain in NSM-CFRP strips is significantly affected by the recycled concrete aggregate; the strain decreases when the RCA percentage increases due to a drop in the bond between CFRP strips and the surrounding concrete. The bond between the NSM-CFRP strips and the concrete cast with natural aggregate is stronger than the bond between the NSM-CFRP strips and the RAC. The reason for the reduction in bond strength is the recycled concrete aggregates consist mostly of cement mortar attached to old virgin aggregate. The mortar itself has lower strength than the virgin aggregate. Using SNSM CFRP in strengthening/repairing specimens significantly reduced the induced strain in NSM-CFRP strips because a larger resisting area available to handle the stresses developed. Fig. 10 shows a comparison between NSM CFRP and SNSM CFRP in terms of strain induced in the CFRP strips.
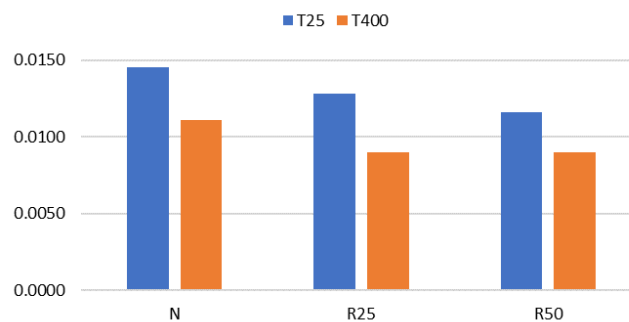

Figure 9. Strain induced in NSM CFRP strips to ultimate vs. temperature for heat-damaged/repaired and unheated/strengthened beams.

Barham, W.S., Obaidat, Y.T., Alkhatatbeh H.A.
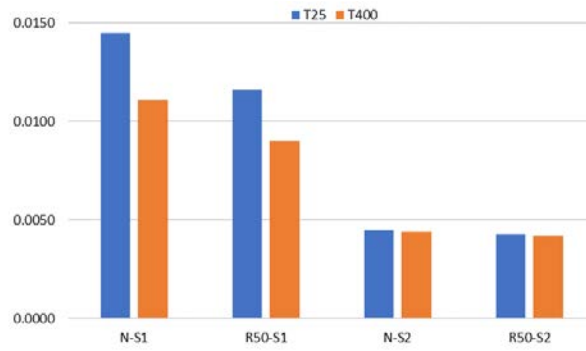
**Figure 10. Strain induced to ultimate vs. temperature
for different strengthening/ repairing configurations.**

3.6.2 Bond Slippage Between Concrete and CFRP strips

Fig. 11 shows that the bond slippage occurred between CFRP strip and surrounding concrete substrates in the first configuration with one strip at the bottom. The slippage is significantly affected by the recycled concrete aggregate. The maximum slippage at ultimate load increases as the RCA content increases due to lower bond strength between CFRP strips and the surrounding concrete because of the large amount of cement mortar attached to the aggregate in RCA. Fig. 12 indicated that using two strips at the sides helps to minimize the slippage to about 40 % of its value in the first configuration (S1) where a single concentrated strip at the bottom is used.
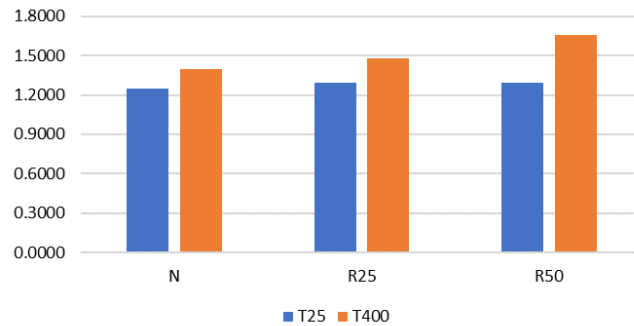
**Figure 11. Bond slippage between NSM CFRP strips vs. temperature
for heat-damaged/repaired and unheated/strengthened beams.**
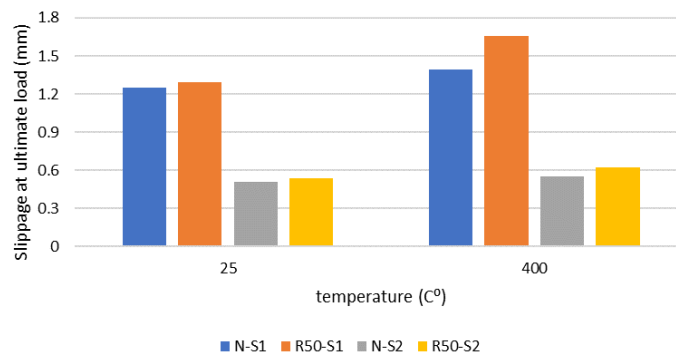
**Figure 12. Bond slippage at ultimate load vs. temperature
for different strengthening/ repairing configurations.**

3.7. Failure modes

Fig. 13 and Fig. 14 show unheated and heat-damaged control beams at failure. All specimens exhibited a flexural mode of failure. Unheated beams, subjected to four-point loading, showed a typical crack propagation as shown in the pictures of Fig. 13. Cracks initiated within the middle of the span at the tension side when the tensile capacity of concrete was reached. By adding further loads, shear cracks appeared diagonally near the supports in the high shear zones and more flexural cracks became visible and extended to the compression side until failure load. Generally, for the same grade of concrete, the recycled aggregate content did not affect the cracks pattern but reduced the load at which the cracks appeared as the recycled aggregate content increased because the RAC has lower mechanical properties.
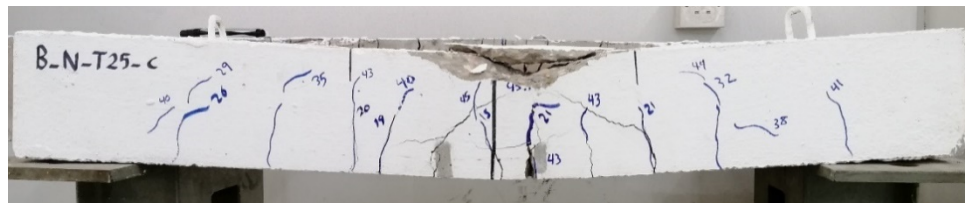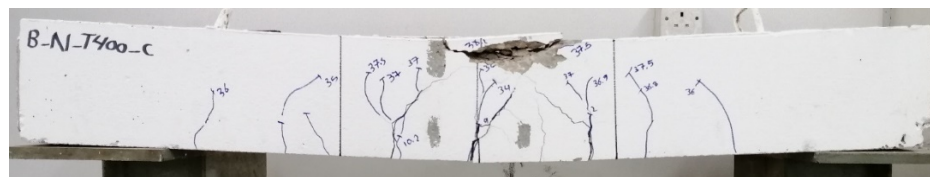
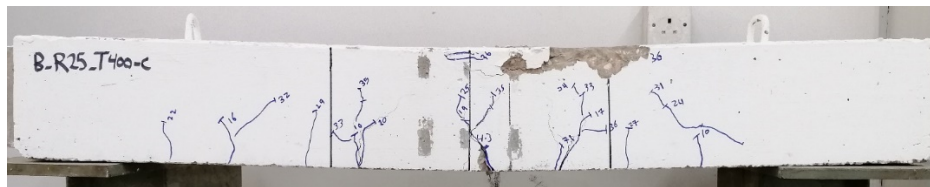**a) B-N-T25-C, Loading cracks**
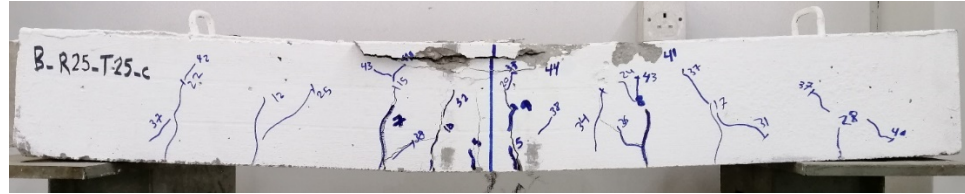
b) B-R25-T25-C, Loading cracks

c) B-R50-T25-C, Loading cracks

Figure 13. Failure mode of unheated control specimens at 25 °C.

For beams damaged at 400ºC, Fig. 14 indicated that failure mode and cracking patterns are similar to those of unheated beams, Cracks initiated at straight vertical profiles in the middle of span in the tension zone before diagonal cracks appeared near the supports. Then more cracks appeared and extended to the compression side, leading to failure. Specimens failed by yielding of tensile steel and then compression failure in concrete at the compression zone with an increase in the number of cracks.

a) B-N-T400-C, Loading cracks
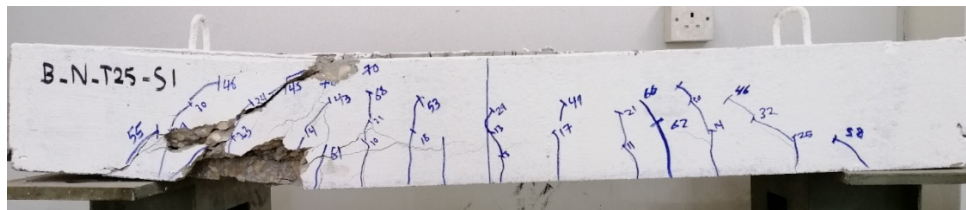

b) B-R25-T400-C, Loading cracks

c) B-R50-T400-C, Loading cracks

**Figure 14. Failure mode of control test specimens heated at 400ºC for 3 hrs.**

The failure modes of intact specimens strengthened with one NSM-CFRP strip at the bottom are shown in Fig. 15. For specimens B-N-T25-S1, B-R25-T25-S1, B-R50-T25-S1, and B-R100-T25-S1, when the load applied, flexural cracks initiated at the middle zone, and with further application of the load, diagonal cracks initiated near supports in the high shear zone with inclination before the cracks propagated rapidly toward the high-stress zone. Near ultimate load, horizontal cracks at the web appeared and caused a cover separation. The collapse of the beams started with partial concrete cover separation followed by

shear failure. On the other hand, specimens strengthened with SNSM CFRP Strips (two strips, one strip at each side), B-N-T25-S2 and B-R50-T25-S2, at ultimate stage, failed by the horizontal cracks that appeared and caused cover separation and then flexural failure followed by concrete crushing. The collapse of the beams started with partial concrete cover separation followed by concrete crushing.
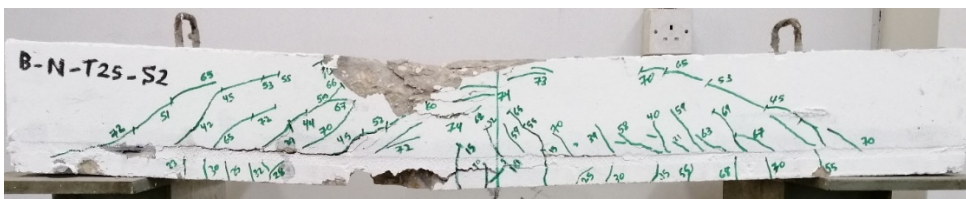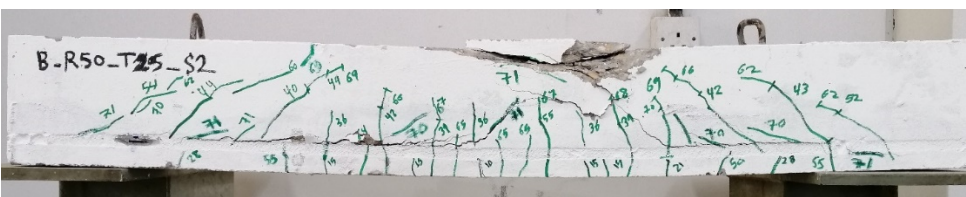

a) B-N-T25-S1, Loading cracks
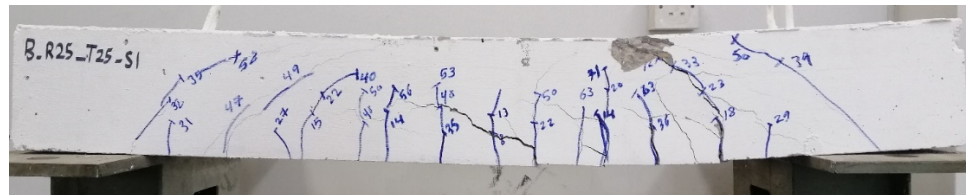
b) B-R25-T25-S1, Loading cracks
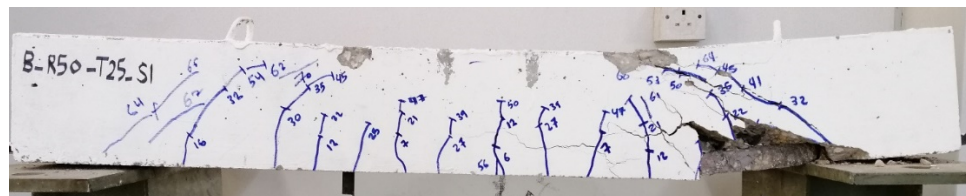
c) B-R50-T25-S1, Loading cracks
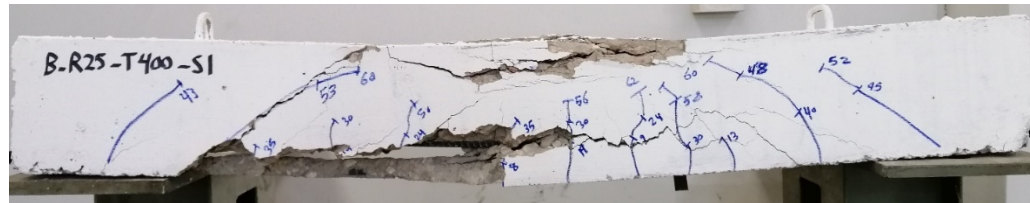

d) B-N-T25-S2, Loading cracks

e) B-R50-T25-S2, Loading cracks

**Figure 15. Failure mode of strengthened specimens at 25 °C.**

Specimens that heat-damaged at 400 °C and were repaired with one NSM CFRP strip at the bottom are shown in Fig. 16. For specimens B-N-T400-S1, B-R25-T400-S1, B-R50-T400-S1, and B-R100-T400-S1, when the load applied, flexural cracks were initiated at the middle zone, and with further application of the load, diagonal cracks initiated near supports in the high shear zone with inclination before they propagated rapidly toward the high-stress zone. However, near ultimate load, specimens with different concrete mixes showed different failure modes.
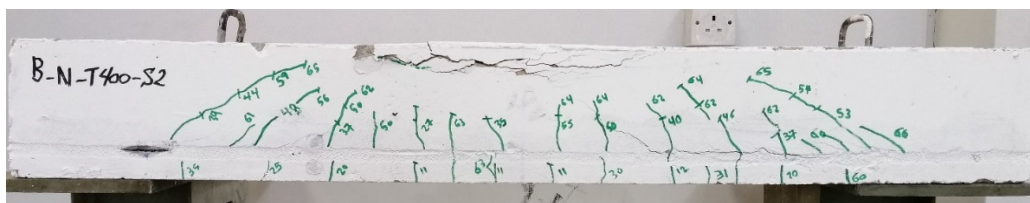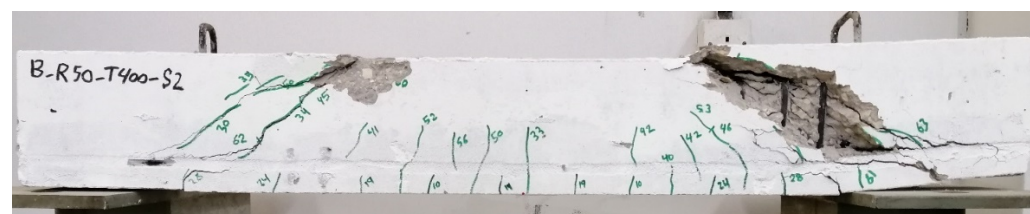
a) B-N-T400-S1, Loading cracks

b) B-R25-T400-S1, Loading cracks
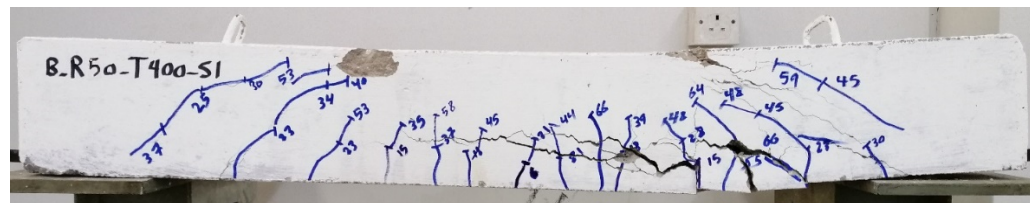
c) B-R50-T400-S1, Loading cracks

d) B-N-T400-S2, Loading cracks

e) B-R50-T400-S2, Loading cracks

Figure 16. Failure mode of repaired test specimens after heating at 400ºC for 3 hrs.

For B-N-T400-S1, partial cover separation with hair-line cracks in the concrete at the compression zone appeared due to concrete crushing. Local splitting of the epoxy cover was noticed. Specimen B-R25-T400-S1 experienced concrete crushing at the same time with partial concrete cover separation. In contrast, B-R50-T400-S1 failed by horizontal cracks that caused partial cover separation followed by shear failure, whereas B-R100-T400-S1 failed by shear. This is because shear capacity is more dependent on concrete than steel in addition to the low shear resistance of RAC as RCA% increases. On the other hand, specimen B-N-T400-S2, repaired with SNSM CFRP Strips (two strips, one strip at each side), failed at the ultimate stage by concrete crushing, whereas B-R50-T400-S2 experienced partial cover separation followed by shear failure. This is because recycled aggregate concrete has a reduction in concrete's mechanical properties including compressive strength and tensile strength in addition to the lower shear resistance of beams cast with RAC.

3.8. Comparison with related work in the literature

The optimum replacement ratio of recycled aggregate to enhance the mechanical properties of concrete was reported in [48] as 30 % while based on the current work is about 25 %. In this study, at 50 % RA replacement ratio, the compressive strength drops significantly at 400 °C while [49] reported significant drop in compressive strength for 30 % replacement ratio at 600 °C. Furthermore, the experimental results obtained in this work is consistent with the findings reported in [14–19, 50, 51]. The recycled aggregate

content slightly affects the load – deflection behavior of reinforced concrete beams. The ultimate load, mid-span deflection, stiffness, and toughness for NA beams is almost comparable to ultimate load for RAC beams at room temperature. Heat damaged beams repaired with NSM-CFRP were found to regain the flexural capacity and increase the load capacity and stiffness of damaged beams. The failure mode of repaired specimens with NSM-CFRP was partial concrete cover separation followed by concrete crushing.

4. Conclusions

Based on this study, and its established conception and formulations, the following conclusions can be drawn:

1. Exposing plain RAC to elevated temperatures of 400 °C for three hours created intense cracking on its surface. The cracks intensity increases as the recycled concrete aggregate increases as well as the level of heat exposure. Accordingly, their post-heating mechanical performance degraded as indicated by the reduction in its strength.

2. Recycled concrete aggregate does not have an effect in the ultimate load carrying capacity of unheated reinforced beams when the compressive strength of concrete is fixed whereas exposing reinforced recycled concrete beams to elevated temperatures of 400°C for three hours causes a noticeable damage and degradation on their post-heating mechanical properties and a bond deterioration between the RAC and the steel reinforcement, as indicated by the reduction in the flexural load capacities and stiffnesses.

3. For heat-damaged beams, the reduction in stiffness increases as RCA content increases due to the large amount of decomposed cement mortar in the RAC that leads to a weaker bond with steel.

4. NSM-CFRP strips technique is suitable for the strengthening/repairing of unheated/heat-damaged, reinforced, recycled aggregate concrete beams.

5. Strengthening of intact beams with NSM CFRP strips helped to improve the overall mechanical performance. Specimens cast with different replacement ratios showed a comparable and typical response, based on the load-deflection curves.

6. The stiffness of the repaired beams decreased as the recycled concrete aggregate content increased due to the weaker bond between damaged recycled aggregate concrete and the epoxy adhesive.

7. Using side NSM CFRP with two strips at sides (one strip at each side) for strengthening and repairing of intact/heat-damaged RAC beams helps to achieve slightly higher load carrying capacities

8. The SNSM CFRP strips repairing configuration helps to reduce the induced strain in the CFRP strips to about 40 % of its value when a single concentrated strip at bottom is used. Moreover, it helps to minimize the slippage due to lower stresses and strains in the CFRP strips.

5. Acknowledgement

References

1. El-Nimri, R., Abdel-Jaber, M., Hunaiti, Y., Abdel-Jaber, M. Behavior of light-gauge steel beams filled with recycled concrete. Magazine of Civil Engineering. 2021. 10102–10102. DOI: 10.34910/MCE.101.2

2. Bairagi, N.K., Vidyadhara, H.S., Ravande, K. Mix design procedure for recycled aggregate concrete. Construction and Building Materials. 1990. 4(4). Pp.188–193. DOI: 10.1016/0950-0618(90)90039-4

3. De Brito, J., Saikia, N. Recycled Aggregate in Concrete: Use of Industrial. Construction and Demolition Waste. Green Energy and Technology. Springer-Verlag, London. 2013. DOI: 10.1007/978-1-4471-4540-0

4. Kabir, M.I., Subhani, M., Shrestha, R., Samali, B. Experimental and theoretical analysis of severely damaged concrete beams strengthened with CFRP. Construction and Building Materials. 2018. 178. Pp. 161–174. DOI: 10.1016/j.conbuildmat.20-18.05.038

5. Shahidan, S., Azmi, M.A.M., Kupusamy, K., Zuki, S.S.M., Ali, N. Utilizing construction and demolition (C&D) waste as recycled aggregates (RA) in concrete. Procedia engineering. 2017. 174. Pp. 1028–1035. DOI: 10.1016/j.proeng.2017.01.255

6. Rao, M.C. Properties of recycled aggregate and recycled aggregate concrete: effect of parent concrete. Asian Journal of Civil Engineering. 2018. 19(1). Pp. 103–110. DOI: 10.1007/s42107-018-0011-x

7. Salahuddin, H., Nawaz, A., Maqsoom, A., Mehmood, T. Effects of elevated temperature on performance of recycled coarse aggregate concrete. Construction and Building Materials. 2019. 202. Pp. 415–425. DOI: 10.1016/j.conbuildmat.2019.01.011

8. Salau, M.A., Oseafiana, O.J., Oyegoke, T.O. Effects of Elevated Temperature on Concrete with Recycled Coarse Aggregates. In IOP Conference Series: Materials Science and Engineering. 2015. (Vol. 96, No. 1, p. 012078). IOP Publishing. DOI: 10.1088/1757-899X/96/1/012078

9. Sarhat, S.R., Sherwood, E.G. Residual mechanical response of recycled aggregate concrete after exposure to elevated temperatures. Journal of Materials in Civil Engineering. 2012. 25(11). Pp. 1721–1730. DOI: 10.1061/(ASCE)MT.1943-5533.00-00719

Barham, W.S., Obaidat, Y.T., Alkhatatbeh H.A.

10. Yang, H., Lv, L., Deng, Z., Lan, W. Residual compressive stress-strain relation of recycled aggregate concrete after exposure to high temperatures. Structural Concrete. 2017. 18(3). Pp. 479–486. DOI: 10.1002/suco.201500153

11. Vieira, J.P.B., Correia, J.R., De Brito, J. Post-fire residual mechanical properties of concrete made with recycled concrete coarse aggregates. Cement and Concrete Research. 2011. 41(5). Pp. 533–541. DOI: 10.1016/j.cemconres.2011.02.002

12. Zega, C.J., Di Maio, A.A. Recycled concrete exposed to high temperatures. Magazine of Concrete Research. 2006. 58(10). Pp. 675–682. DOI: 10.1680/macr.2006.58.10.675

13. Xiao, J.Z., Zhang, C.Z. Fire damage and residual strengths of recycled aggregate concrete. In Key Engineering Materials. 2007. (Vol. 348, Pp. 937–940). Trans Tech Publications. DOI: 10.4028/www.scientific.net/KEM.348-349.937

14. Wardeh, G., Ghorbel, E. Experimental Investigation and Analytical Study on the Flexural Behavior of Reinforced Recycled Aggregate Concrete Beams. Journal of Modern Mechanical Engineering and Technology. 2018. 5. Pp. 1–23. DOI: 10.15377/2409-9848.2018.05.1

15. Knaack, A.M., Kurama, Y.C. Service-load deflection behavior of reinforced concrete beams with recycled concrete aggregate. In Structures Congress 2013: Bridging Your Passion with Your Profession. 2013. Pp. 2705–2716. DOI: 10.1061/978078-4412848.235

16. Ignjatović, I.S., Marinković, S.B., Mišković, Z.M., Savić, A.R. Flexural behavior of reinforced recycled aggregate concrete beams under short-term loading. Materials and structures. 2013. 46(6). Pp. 1045–1059. DOI: 10.1617/s11527-012-9952-9

17. Pan, L.Y., Shao, W.J., Li, G.X., Li, H.F. Experimental Study on Flexural Resistance of Reinforced Recycled-concrete Beams. In Applied Mechanics and Materials. 2013. (Vol. 438, Pp. 789–793). Trans Tech Publications. DOI: 10.4028/www.scientific.net/AMM.438-439.789

18. Sato, R., Maruyama, I., Sogabe, T., Sogo, M. Flexural behavior of reinforced recycled concrete beams. Journal of Advanced Concrete Technology. 2007. 5(1). Pp. 43–61. DOI: 10.3151/jact.5.43

19. Knaack, A.M., Kurama, Y.C. Behavior of reinforced concrete beams with recycled concrete coarse aggregates. Journal of Structural Engineering. 2014. 141(3). p. B4014009. DOI: 10.1061/(ASCE)ST.1943-541X.0001118

20. Duy, N.P., Anh, V.N., Hiep, D.V., Anh, N.M.T. Strength of concrete columns reinforced with Glass fiber reinforced polymer. Magazine of Civil Engineering. 2021: 10108–10108. DOI: 10.34910/MCE.101.8

21. Al-Rousan, R., Abo-Msamh, I. Impact of anchored CFRP on the torsional and bending behaviour of RC beams. Magazine of Civil Engineering. (2020). DOI: 10.18720/MCE.96.7

22. Kozinetc, K.G., Kaarki, T., Barabanshchikov, Y.G., Lahtela, V., Zotov, D.K. Mechanical Properties Of Sustainable Wooden Structures Reinforced With Basalt Fiber Reinforced Polymer. Magazine Of Civil Engineering. 2020. 100(8). Article No. 10012. DOI: 10.18720/Mce.100.12

23. Salakhutdinov, M.A., Gimranov, L.R. Kuznetsov, I.L., Fakhrutdinov, A.E., Nurgaleeva, L.M. PFRP structures under the predominately short term load. Magazine of Civil Engineering. 2020. DOI: 10.18720/MCE.96.1

24. Al-Rousan, R. Behavior of strengthened concrete beams damaged by thermal shock. Magazine of Civil Engineering (2020). DOI: 10.18720/MCE.94.8

25. Travush, V., Konin, D., Krylov, A. Strength of reinforced concrete beams of high-performance concrete and fiber reinforced concrete. Magazine of Civil Engineering. 2018. DOI: 10.18720/MCE.77.8

26. Szabó, Z.K., Balázs, G.L. Near surface mounted FRP reinforcement for strengthening of concrete structures. Periodica Polytechnica Civil Engineering. 2007. 51(1). Pp. 33–38. DOI: 10.3311/pp.ci.2007-1.05

27. Khalifa, A.M. Flexural performance of RC beams strengthened with near surface mounted CFRP strips. Alexandria Engineering Journal. 2016. 55(2). Pp. 1497–1505. DOI: 10.1016/j.aej.2016.01.033

28. Hassan, T., Rizkalla, S. Investigation of bond in concrete structures strengthened with near surface mounted carbon fiber reinforced polymer strips. Journal of composites for construction. 2003. 7(3). Pp. 248–257. DOI: 10.1061/(ASCE)1090-0268(2003)7:3(248)

29. Täljsten, B., Carolin, A., Nordin, H. Concrete Structures Strengthened with near Surface Mounted Reinforcement of CFRP. Advances in Structural Engineering. 2003. 6(3). Pp. 201–213. DOI: 10.1260/136943303322419223

30. De Lorenzis, L., Nanni, A., La Tegola, A. Flexural and Shear Strengthening of Reinforced Concrete Structures with Near Surface Mounted FRP Rods. Proceedings of the 3rd International Conference on Advanced Composite Materials in Bridges and Structures (ACMBS III). 2000. Ottawa. Ontario. Canada. Aug. 15-18. Pp. 521–528.

31. El-Hacha, R., Rizkalla, S., Kotynia, R. Modeling of reinforced concrete flexural members strengthened with near-surface mounted FRP reinforcement. In 7th Int. Symp. on Fiber Reinforced Polymer (FRP) Reinforcement for Concrete Structures (FRPRCS-7). 2005. (Pp. 1681–1700).

32. Al-Mahmoud, F., Castel, A., François, R., Tourneur, C. Strengthening of RC members with near-surface mounted CFRP rods. Composite Structures. 2009. 91(2). Pp. 138–147. DOI: 10.1016/j.compstruct.2009.04.040

33. De Lorenzis, L. and Teng, J.G. Near-surface mounted FRP reinforcement: An emerging technique for strengthening structures. Composites Part B: Engineering. 2007. 38(2). Pp. 119–143. DOI: 10.1016/j.compositesb.2006.08.003

34. Teng, J.G., de Lorenzis, L., Wang, B., Li, R., Wong, T.N., Lam, L. Debonding failures of RC beams strengthened with near surface mounted CFRP Strips. Journal of composites for construction 2006. 10. no. 2. 92–105. DOI 10.1061/(ASCE)1090-0268;10:2-(92). DOI: 10.1061/(ASCE)1090-0268(2006)10:2(92)

35. Yost, J.R., Gross, S.P., Dinehart, D.W., Mildenberg, J.J. Flexural behavior of concrete beams strengthened with near-surface-mounted CFRP strips. ACI Structural Journal. 2007. Vol. 104. Iss. 4. Pp. 430–437.

36. Ferrari, V.J., de Hanai, J.B., de Souza, R.A. Flexural strengthening of reinforcement concrete beams using high performance fiber reinforcement cement-based composite (HPFRCC) and carbon fiber reinforced polymers (CFRP). Construction and Building Materials. 2013. 48. Pp. 485–498. DOI: 10.1016/j.conbuildmat.2013.07.026

37. Jadooe, A., Al-Mahaidi, R., Abdouka, K. Behaviour of heat-damaged partially-insulated RC beams using NSM systems. Construction and Building Materials. 2018. 180. Pp. 211–228. DOI: 10.1016/j.conbuildmat.2018.05.279

38. Jadooe, A., Al-Mahaidi, R., Abdouka, K. Performance of heat-damaged partially-insulated RC beams strengthened with NSM CFRP strips and epoxy adhesive. Construction and Building Materials. 2018. 159. Pp. 617–634. DOI: 10.1016/j.conbuildmat.2017.11.020

39. ASTM, A. C127 Standard Test Method for Relative Density (Specific Gravity) and Absorption of Coarse Aggregate. American Society for Testing and Materials: West Conshohocken, PA, USA. 2015. DOI: 10.1520/C0127-15

40. ASTM, A. C128 Standard Test Method for Relative Density (Specific Gravity) and Absorption of Fine Aggregate. American Society for Testing and Materials: West Conshohocken, PA, USA. 2015. DOI: 10.1520/C0128-15

41. ASTM, C136/C136M-14. (2014). Standard Test Method for Sieve Analysis of Fine and Coarse Aggregates. West Conshohocken, PA, USA. 2014. DOI: 10.1520/C0136-06

42. ASTM C131 / C131M-20. Standard Test Method for Resistance to Degradation of Small-Size Coarse Aggregate by Abrasion and Impact in the Los Angeles Machine, ASTM International, West Conshohocken, PA. 2020. DOI: 10.1520/C0131_C0131M-20

43. ASTM A370-16. Standard Test Methods and Definitions for Mechanical Testing of Steel Products. American Society for Testing and Materials International, West Conshohocken, United States. 2016. DOI: 10.1520/A0370-20

44. ACI Manual of Concrete Practice. Standard practice for selecting proportions for normal, heavyweight, and mass concrete (ACI 211.1), Part I: Materials and General Properties of Concrete, Detroit, Michigan. 2008.

45. ASTM, C143/C143M. Standard Test Method for Slump of Hydraulic Cement Concrete. West Conshohocken, PA. 2000. DOI: 10.1520/C0143_C0143M-00

46. American Society for Testing and Materials International (ASTM). West Conshohocken, PA: 2004.

47. American Concrete Institute. Building Code Requirements for Structural Concrete and Commentary (ACI-318), Farmington Hills, Michigan. 2019. DOI: 10.14359/51716937.

48. Ali, R., Hamid, R. Workability and Compressive Strength of Recycled Concrete Waste Aggregate Concrete. Applied Mechanics and Materials. 2015. 754–755, 417–420. DOI: 10.4028/www.scientific.net/amm.754-755.417

49. Salau, M.A., Oseafiana, O.J., Oyegoke, T.O. Effects of Elevated Temperature on Concrete with Recycled Coarse Aggregates. IOP Conference Series: Materials Science and Engineering. 2015. 96, 012078. DOI: 10.1088/1757-899x/96/1/012078

50. Jadooe, A., Al-Mahaidi, R., Abdouka, K. Experimental and numerical study of strengthening of heat-damaged RC beams using NSM CFRP strips. Construction and Building Materials. 2017. 154. Pp. 899–913. DOI: /10.1016/j.conbuildmat.2017.07.202

51. Seara-Paz, S., González-Fonteboa, B., Martínez-Abella, F., Eiras-López, J. Flexural performance of reinforced concrete beams made with recycled concrete coarse aggregate. Engineering Structures. 2018. 156, 32–45. DOI: 10.1016/j.engstruct.20-17.11.015

Information about authors:

Wasim Barham, PhD
ORCID: https://orcid.org/0000-0003-1106-5195
E-mail: wsbarham@just.edu.jo

Yasmeen Obaidat, PhD
ORCID: https://orcid.org/0000-0002-0533-366X
E-mail: ytobeidat@just.edu.jo

Huthaifa Alkhatatbeh,
ORCID: https://orcid.org/0000-0002-3017-1834
E-mail: haalkhatatbeh16@eng.just.edu.jo